Contents lists available at ScienceDirect

Talanta

journal homepage: www.elsevier.com/locate/talanta

Programmable flow injection in batch mode: Determination of nutrients in sea water by using a single, salinity independent calibration line, obtained with standards prepared in distilled water

Mariko Hatta [a,b,*], Jaromir (Jarda) Ruzicka [a], Christopher I. Measures [a], Madeline Davis [a]

[a] Institute of Arctic Climate and Environmental Research, Japan Agency for Marine-Earth Science and Technology, Institute of Arctic Climate and Environmental Research
[b] University of Hawaii, 1000 Pope Road, Honolulu, HI, 96822, USA

ARTICLE INFO

Keywords:
Programmable flow
Nutrients
Sea water
Schlieren effect
Flow-batch mode

ABSTRACT

Interference of the Schlieren effect on sea water analysis by spectrophotometry is caused by the flow of solutions of different ionic strengths through a flow cell. A flow injection assay protocol programmed in a flow-batch format removes this interference and allows the use of a calibration line, obtained in deionized water, for determination of analytes in sea water samples of different salinity. This Single Line Calibration (SLC) technique is validated on the most frequently performed nutrient assays. Automated determinations, performed at rates ranging from 20 to 60 samples/hr, covered seawater sample ranges from nM to mM with limits of detection: 12 nM for nitrite, 94 nM for nitrate, 47 nM for phosphate, and 240 nM for silicate. Reproducibility of the determinations was equal to or better than, 3% r.s.d. and day to day calibration was within 10%. The programmable FI, uses about 1/5th volume of reagents compared to continuous flow techniques.

1. Introduction

The goal of this communication is to present the concept of a programmable Flow Injection (pFI) in Batch mode (FIB), and use it to optimize the determination of the nutrients (nitrite, nitrate, phosphate, and silicate) in sea water of variable salinity. The *Introduction* of this work comprises three parts: the principle of the FIB technique, its instrumentation, and its application to research in chemical oceanography. *Results and Discussion* presents the data obtained by FIB from analyzing nutrients in standards prepared in deionized water (DI) and sea water (SW) and shows the correlation of the results obtained by DI and SW calibrations. In the *Conclusion*, the performance of FIB is compared with continuous flow techniques (FIA and air-segmented flow) in resolving the salinity issue, as well as carryover, baseline drift, reagent consumption, and manifold configuration.

1.1. Batch and flow based analytical techniques

Prior to the advent of continuous flow analysis, all reagent-based assays were performed in a batch mode. Each sample (and standard solution) was assigned an individual container into which samples and reagents were metered, thoroughly mixed, and left to react until chemical equilibrium was reached. For a spectrophotometric measurement, the reaction mixture was transferred into a cuvette for the absorbance measurement. Besides analytical applications, molar absorptivities, dissociation constants, stability constants, and other coefficients have also been determined in a batch mode. Obviously, a batch mode is labor-intensive, and the manual handling is prone to error, and automation of batch assays requires complex (robotic) instrumentation.

This is why a majority of reagent-based assays have been automated in a flow-based format, such as Flow Injection (FI) analysis [1,2]. However, inevitably, the continuous flow format also has limitations:

- Assay protocols are more difficult to optimize because the response of a FI system is based on the *concentration gradient* of the sample formed within a moving stream of reagent. In batch mode known volumes of sample and reagent solutions are mixed to obtain *a single homogeneous solution with a known concentration* of components.
- Since the response in the FI mode is a result of the combination of the physical process of dispersion of the sample and the chemical process

* Corresponding author. Institute of Arctic Climate and Environmental Research, Japan Agency for Marine-Earth Science and Technology, Yokosuka, 237-0061, Japan.
E-mail addresses: mhatta@jamstec.go.jp (M. Hatta), jardahawaii@gmail.com (J.(J. Ruzicka), measures@hawaii.edu (C.I. Measures), davismn@hawaii.edu (M. Davis).

https://doi.org/10.1016/j.talanta.2021.122354
Received 28 January 2021; Received in revised form 16 March 2021; Accepted 17 March 2021

of the formation of the resulting analyte species, it is difficult to determine whether equilibrium was reached, while in batch mode a steady-state response confirms that the chemical reactions reached equilibrium.

- Spectrophotometric measurement on a flowing solution is also affected by the Schlieren effect which is caused by the transition of solutions of different ionic strength through the flow cell [3–6]. In contrast, there is no Schlieren effect interference when measuring a stationary homogenous mixture.

For the majority of FI applications, these obstacles and drawbacks can be successfully overcome as documented in over 23,000 FI-based methods published to date [7]. However, among these publications, there are almost 200 papers, termed "flow-batch systems" designed to analyze samples of high viscosity. The common component of all of these continuous flow systems is that they have a mixing chamber equipped with a stirring bar. The drawback of this design is the large volume of the chamber and continuous flow operation, which increases sample and reagent consumption. Also, this design does not function as a traditional batch method, because while the sample and reagents are homogenized by stirring, the spectrophotometry is still performed on a flowing solution and does not eliminate the Schlieren effect. The Schlieren effect is a unique issue to flow systems. It is caused by lenses that form between sample/reagent and carrier segments of different refractive index that result from the parabolic geometry formed at the interfaces under laminar-flow conditions while the solution is flowing and that these lenses are then carried through the flow cell distorting the optical signal during their passage.

1.2. Flow injection in batch mode

To replicate the conditions of a traditional batch assay three conditions must be fulfilled:

- The assay cycle has to be programmed to comprise of two sections: sample *processing* performed in a *flow* mode, while subsequent sample *monitoring* is performed in a *batch* mode. Sample processing includes sample dilution, metering of sample and reagent(s) in well-defined proportions, their homogenous mixing, heating, and transport into the flow cell. Monitoring is then performed on this *homogenous* mixture of sample and reagents, while it is arrested within the flow cell.
- The flow cell must be filled *through its entire length* with a reaction mixture *of uniform composition.* To avoid the inevitable dilution by the carrier with the reaction mixture at its leading and trailing edges, this can only be achieved if the volume of the reaction mixture is equal to, or larger than, five times the volume of the conduit between the confluence point where the reagents and sample meet and the end of the optical path of the flow cell [8,9]. Therefore, the flow system has to be designed in such a way that the volume of this conduit (equal to the channel and the flow cell volumes, shown in Fig. 1, green and yellow line) is minimized, as otherwise, the volume of the reaction mixture will have to be very large, and therefore difficult to flush from the system between the assays. Such a construct is achieved by using a lab-on-valve (LOV) platform [10,11] equipped with a Linear Light Path (LLP) flow cell [12,13] (Fig. 2) where the volume of the connecting channel (Fig. 1, dark green line) between the confluence point and the flow cell is minimized.
- Absorbance values used for the construction of the calibration line are collected when the chemical reactions are close to, or at steady state.

A simple way to show this for a single reagent assay protocol using BTB dye is described below (Figs. 3 and 4):

The assay protocol comprises a flow-based section where sample and reagent(s) are being processed (*the flow section*, Fig. 3 steps 1 and 2) and a batch section where the stopped reaction mixture is monitored (*batch section*, Fig. 3 step 3). The *flow section* of the FIB protocol comprises:

- Step 1: a sample (BTB dye, blue) is aspirated by pump 1 into the holding coil 1 (HC1).
- Step 2: the sample is transferred into holding coil 2 (HC2) simultaneously with a reagent (buffer, grey), which is added at the confluence point. The mixing ratio of the sample with the reagent (S+R=1+1) is controlled by combining the delivery rate from HC1 (set by pump 1, P1) with the aspiration rate into HC2 (set by pump 2, P2).

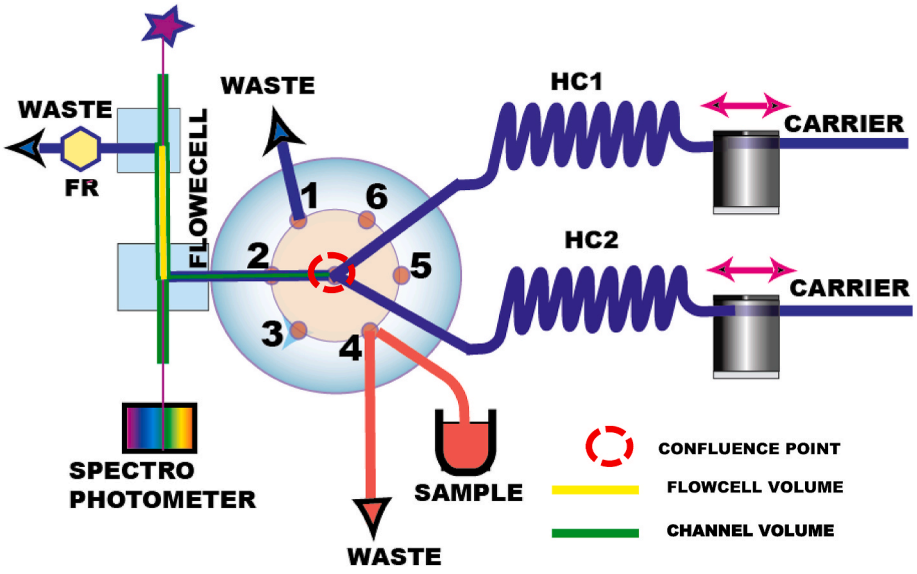

Fig. 1. Lab-on-valve manifold for programmable Flow Injection. HC1 and HC2 – holding coils, 1–6 ports. FR-flow restrictor.

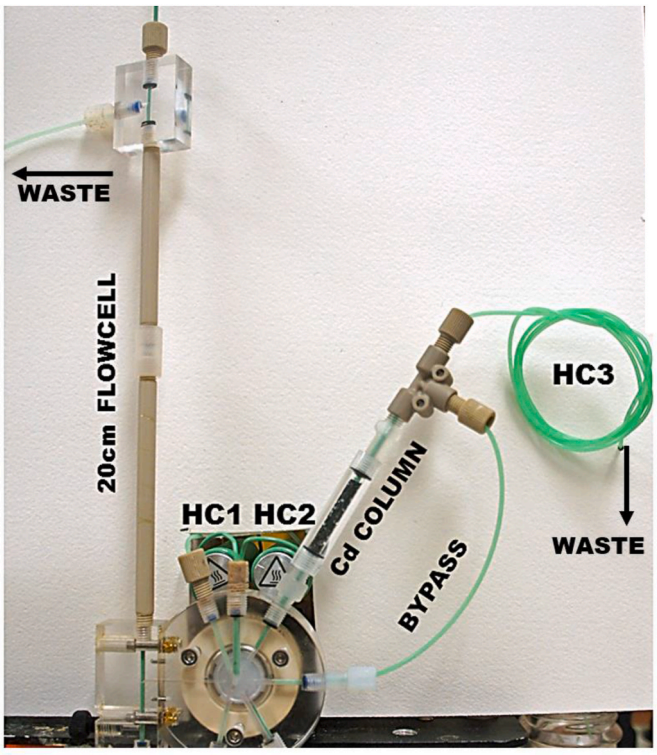

Fig. 2. Lab-on-valve instrument equipped with 20 cm long flow cell, configured for nitrate assay. HC1, HC2, HC3 holding coils. (For details see text).

- Step 3: the sample and the reagent mixture (light blue) is transferred from HC2, through the confluence into the flow cell by a forward flow that delivers a transfer volume (TRv) calculated to place the centroid of the mixture into the middle of the light path of the flow cell.

In the *batch section* of the protocol, the mixture is arrested within the flow cell while absorbance data are collected from the stationary solution. The duration of the stop-flow period is designed to stabilize movement of the solution within the flow cell, and to provide a sufficient incubation time for the reagent-based assays to be close to or at steady state.

1.3. Advances in instrumentation

Carrying out novel ideas critically depends on the availability of the key hardware and software components, and therefore it took so long to bring the rather obvious idea of FIB to fruition. The *milliGAT pumps* which are crucial components of a reliable flow programming are based on a unique, ingenious design of four pistons moving on a rotating cam, where one piston is filling, one is delivering, and the other two pistons are moving between the filling and emptying ports [14]. Conceived by Duane Wolcott in 1995, patented in 2002 [15], it took another 15 years to develop milliGAT pump into a reliable commercial product. The *LOV manifold* which was conceived in 2000 [10], and evolved into the present design with an interchangeable flow cell, only became commercially available five years ago. The *LLP* flow cell invented fifteen years ago by G. Klein, lingered in obscurity until recently when its performance was investigated and compared with widely used Liquid Core Waveguide (LCW) flow cell [12]. These hardware components combined with supporting software only recently coalesced into a commercially available instrument which makes pFI a practical tool for research in chemical oceanography. Miniaturization of the flow path in the LOV format is the critical feature of the instrument, where the confluence point is a hub interconnecting bidirectional milliGAT pumps (Fig. 1), the holding coils (HC1, HC2), and the peripheral ports (port 1–6 in the LOV format) that accommodate a flow cell (port 2), a sample inlet (port 4), and reagent ports (ports 3, 5, and 6). The key feature of the flow path (Fig. 2), is its low internal volume and uniform internal diameter of the channel including the light path of the flow cell (Fig. 1, dark and light green lines, 0.8 mm I.D, with a total volume of 120 μL). This internal volume requires only 600 μL of a reaction mixture and a transfer volume (TRv) of 300–400 μL to establish the necessary batch conditions within the flow cell during the stop flow period.

Our previous work documented the advantages of programmable FI for the trace determination of nutrients in sea water [12,16–18]. In this work, the flow-batch variant is introduced and developed to verify the concept of the incorporation of a Single Line Calibration (SLC) method for the determination of nutrients in sea water. This novel concept enables the use of a calibration line, obtained with standards prepared in DI water, to be used to calculate the values of sea water samples.

1.4. Application of flow-batch technique on chemical oceanography

In this study, we aim at resolving two issues that impede analysis of

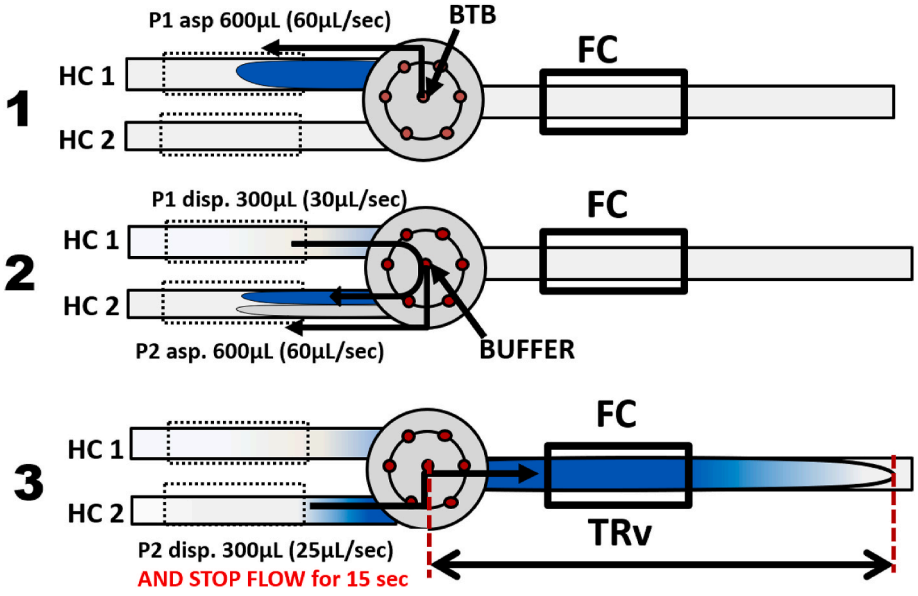

Fig. 3. Flow sequence used for verification and optimization of a batch-flow concept is also suitable for single reagent assay.

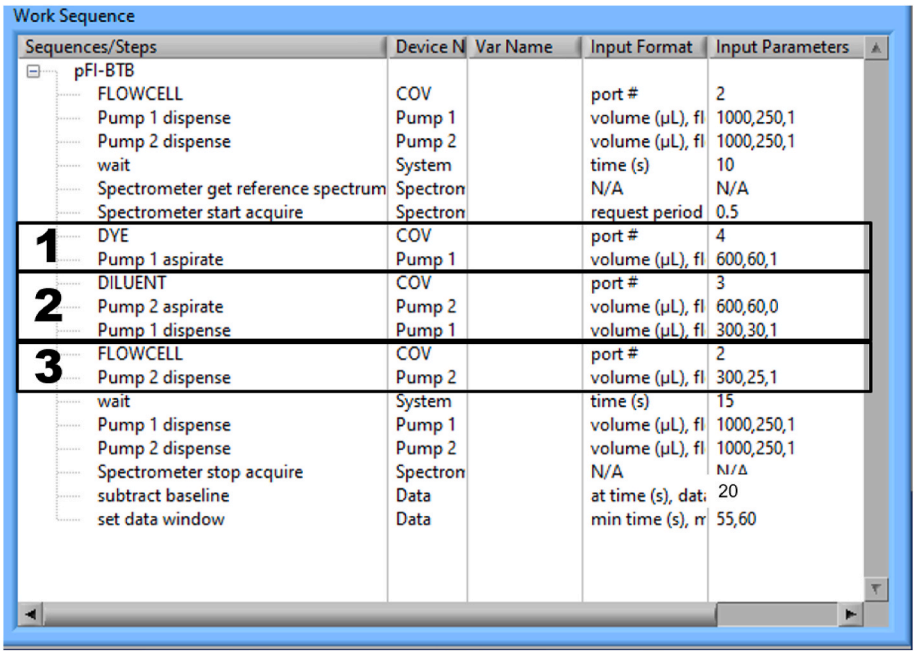

Fig. 4. Assay protocol for single reagent assay. The steps correspond to steps in the flow sequence shown in Fig. 3.

sea water samples: 1) Schlieren effect that distorts absorbance measurement and 2) effect of salinity that causes differences in calibrations obtained in DI and in sea water samples as well as samples collected in estuaries.

In the ocean, salinity can vary from a few psu (practical salinity units, roughly equivalent to grams of total dissolved salts per kg of solution) in coastal waters to 35 psu in the open ocean, which requires careful salinity matching of the standard solutions during the analysis. Therefore, oceanographic researchers need a supply of low nutrient seawater (LNSW) to produce salinity matched standards which can be difficult to obtain for labs that do not have easy access to open ocean low nutrient areas. While LNSW can be generated from nutrient-rich regions this requires a time-consuming process of letting existing natural biological processes reduce the nutrient levels within the containers. In addition to the collection problem, once obtained the LNSW must be filtered to prevent the (further) growth of organisms and then stored in the dark for significant periods of time. Last, but not least, the LNSW prepared collected at different locations and prepared by different methods may differ in composition at the trace level. Therefore, the use of DI water to perform calibration and its use as a carrier solution will eliminate these issues by serving as uniform, widely available matrix.

2. Experimental

2.1. Instrumentation

The instrument, miniSIA-2 (Global FIA, Fox Island, WA, USA), comprises two high precision, synchronously refilling milliGAT pumps, two thermostated holding coils, a 6-port LOV (model COV-MANI-6, constructed from polymethyl methacrylate, Perspex®) furnished with a module for an external flow cell. All tubing connections, downstream from the milliGAT pumps including the holding coils (volume 1000 µL), were made with 0.8 mm I.D. polytetrafluoroethylene (PTFE). The holding coils were thermostated at 25 °C for all experiments unless stated otherwise. The tubing between the carrier stream reservoirs and the milliGAT pump was made from 1.6 mm I.D. PTFE tubing to minimize degassing under reduced pressure at higher aspiration flow rates. A spectrophotometer (USB 4000 or Flame, Ocean Insight, Orlando, FL, USA) and a light source were connected to the flow cells by using optical fibers with 500-µm silica cores encased in 0.8 mm I.D. green PEEK tubing. The end of each fiber exposed to the liquid was cemented with epoxy, cut square, and polished. An Ocean Optics Tungsten Halogen (HL-2000, Ocean Insight, Orlando, FL, USA) light source was used. All assay steps were computer-controlled using commercially available software (FloZF, GlobalFIA, Fox island, WA, USA).

The LLP flow cell (Fig. 2) can be purchased from Global FIA, ours was constructed in house [12,13]. The outlet of the LLP flow cell, was fitted with a 40-psi flow restrictor (GlobalFIA, Fox Island, WA, USA), which, by elevating the pressure within the flow path, efficiently prevented the formation of microbubbles from spontaneous outgassing.

2.2. Reagents and materials

2.2.1. Water

DI was prepared using an Elix Type 2 Pure Water Systems, and then passed through a Milli-Q Integral Water Purification Systems (Merck Millipore, Massachusetts, USA.). DI water was stored overnight to allow excess dissolved air to equilibrate at atmospheric pressure to minimize microbubble formation within the flow channel.

SW used for the preparation of all sea water standards was collected at the Hawaii Ocean Time-series station ALOHA (22°45′N, 158°W), in the North Pacific Ocean, and was filtered through a 0.45 µm filter (Supor 450 Membrane filter, Pall), and was stored in the dark.

2.2.2. Dye experiment

Carrier: 10 times diluted borax/carbonate buffer stock solution.

Diluted borax/carbonate buffer, pH=9.2 was prepared by dissolving 19 g of Sodium Tetraborate Decahydrate ($Na_2B_4O_7 \cdot 10H_2O$,S248-500, CAS 1303-96-4, certified ACS, Fisher Scientific) in 1 L of DI water and by dissolving 5.3 g Sodium Carbonate (Na_2CO_3, S263-500, CAS 497-19-8, certified ACS, Fisher Scientific) in 1L of DI water. These stock solutions are mixed in proportion 3+1 of borax and carbonate, and then diluted 10x with DI water for use as solvent for preparation of the BTB stock and standard solutions.

176.3 µM Bromo Thymol Blue (BTB) stock solution was prepared by dissolving 0.077 g of BTB powder ($C_{27}H_{28}Br_2O_5S$, m.w. 624. CAS 34722-90-2) in 700 mL of diluted borax/carbonate buffer stock solution, and was further diluted daily to obtain working standards (0–529 nM) in the diluted buffer solution.

2.2.3. Nitrite and nitrate

Carrier solution: For the nitrite assay DI water was used as a carrier. For the nitrate assay, DI water was used in P1 and buffer solution was used in P2 .

Buffer solution for the nitrate assay was 0.05 M ammonium chloride (NH_4Cl, CAS: 12125-02-09, Fisher Scientific), the pH of which was adjusted to 8.5 with 2.5 M sodium hydroxide (NaOH, CAS: 1310-73-2, Fisher Scientific).

Nitrite and nitrate standards were prepared by dilution with DI water, or with sea water, from 1000 ppm commercial standards (EXAXOL, Clearwater, FL, USA). The 100 μM N standard solution was prepared weekly, the 0–10 μM N standards daily.

For the assay of nitrate, the Gries reagent was prepared by adding 4.0 mL concentrated sulfuric acid (H_2SO_4) to 96 mL of DI water. Next, 2.0 g sulphanilamide (S9251-100G, CAS: 63-74-1, Sigma-Aldrich, Massachusetts, USA) was added and dissolved, followed by 50 mg n-(1-Naphthyl) ethylene amine dihydrochloride (222488-10G, CAS: 1465-25-4, Sigma-Aldrich, Massachusetts, USA). Stored in darkness, this solution was stable for four weeks. For the assay of nitrite, the Gries reagent was diluted 1+1 with a H_2SO_4 solution (4.0 mL concentrated H_2SO_4 diluted in 96 mL of DI water).

The Plexiglass reduction column was made by Global FIA. Dimensions 3.0 mm I.D. 30 mm long. It was filled with Cd granules which are held in the column by green PEEK tubing (1/16″ O.D. (1.6 mm) x 0.03" I.D.(0.8 mm), IDEX Health & Science, LLC, Oak Harbor, WA, USA with appropriate fittings and O-rings. The downstream end of the column was fitted with 1 m long 0.8 mm I.D. flexible tubing serving as a holding coil (HC3) leading to waste and by a bypass made of 0.8 mm I.D. tubing (Fig. 2).

Column preparation, activation, and maintenance: Mount the column filled with Cd metal (granulated mesh 20 to 60 GFS Chemicals 800 Kaderly Dr. Columbus OH 43228) on port # 6 of the LOV module (Fig. 2), and flush it with DI water using P1 at a flow rate of 250 μL/s for 2 min. Examine the eluate to ensure there are no Cd particles flushed from the column. Next: 1) place 1 M HCl solution in the end of the HC3 coil (Fig. 2) to aspirate 1 mL of 1 M HCl on to the column, and hold for 4 min, or until the Cd granules become shiny, 2) return the end of the HC3 coil to a waste container, and flush the HCl from the column and rinse with 2 mL of DI carrier using P1, 3) aspirate 1 mL of 3% w/w solution of copper sulfate ($CuSO_4$) and hold on the column for 30 s, the Cd granules will turn black, and then 4) flush with 3 mL of DI water using P1 followed by 3 mL buffer solution using P2. Activation: 1) aspirate 1 mL of 50 μM nitrate (NO_3) standard solution into the column, hold for 2 min. 2) flush with 5 mL buffer using P2. Note that exposure to air will oxidize the Cd/Cu making the reduction inefficient. Therefore, store the column filled with the buffer solution. Additional information on column preparation and maintenance is in a valuable article by Frenzel et al. [19].

2.2.4. Phosphate

2.2.4.1. Carrier solution: DI water. Phosphate stock standards were prepared by diluting a commercial PO_4 standard containing 1000 ppm phosphate standard solution (LC185701, LabChem) in DI water. The 100 μM P stock solution was prepared weekly, and further diluted daily to obtain working standards (0.5 μM–3 μM P) in DI water or sea water.

A phosphate blank solution (to assess Si interference) was spiked with a silica standard solution (360 μM) by adding 1 mL of a commercial silica standard containing 1000 ppm silica standard solution (15747-100ML, Fluka) in 100 mL of DI water. The silica solution had to be neutralized with HCl, because the silica standard is prepared in sodium hydroxide solution (pH12), which must be neutralized to match the pH of the phosphate standard solutions.

Potassium antimony tartrate stock solution (15 mM) was prepared by dissolving 0.45 g of potassium antimony (III) oxide tartrate trihydrate (383376-100G, CAS28300-74-5, Sigma-Aldrich) in 45 mL of DI water. The mixed molybdate reagent was prepared by dissolving 2.0 g of ammonium molybdate tetrahydrate crystalline (A674-500, CAS12054-85-2, certified ACS, Fisher Scientific) in 100 mL of DI water in a 250 mL bottle. Next, 1.6 mL of potassium antimony tartrate stock solution was added, followed by 15 mL of conc. H_2SO_4 (A300-500, CAS7664-93-9, certified ACS, Fisher Scientific). Finally, DI water was added to make a final volume of 200 mL. This solution is stable for one month.

The mixed solution of ascorbic acid and SDS solution was prepared by dissolving 1.2 g of L (+)-ascorbic acid (A15613, CAS50-81-7, Alfa Aesar) in 40 mL of DI water, and then 1.2 g of solid of ultrapure sodium dodecyl sulfate (J75819-22, CAS151-21-3, thermo scientific) was added into the prepared 3% ascorbic acid solution. Note that it is recommended to prepare this solution 30 min before use, in order to stabilize its reducing strength, as otherwise, the slope of calibration line with freshly prepared reagent will be up to 5% steeper than those obtained later. Alternatively, to prevent loss of reducing strength, the solution should be deareated after preparation.

2.2.5. Silicate

2.2.5.1. Carrier solution: DI water. Silicate stock standard containing 3.57 mM Si was prepared weekly by diluting a commercial 1000 ppm Si standard (15747-100ML, Fluka) with 0.5 M HCl. This stock solution was further diluted daily, to obtain working standards (20 μM Si to 300 μM Si) in DI water and sea water. The silica solution had to be neutralized by HCl, because the silica standard is prepared in sodium hydroxide solution (pH12), which must be neutralized to match the pH of DI and SW standard solutions.

The acidified molybdate reagent was prepared by dissolving 1.0 g of ammonium molybdate tetrahydrate crystalline (A674-500, CAS12054-85-2, certified ACS, Fisher Scientific) in 50 mL of DI water. Next, 0.5 mL of conc. sulfuric acid (A300-500, CAS7664-93-9, certified ACS, Fisher Scientific) was added and then DI water was added to make a final volume of 100 mL. This solution was stable for one month.

The mixed solution of ascorbic acid and SDS solution was prepared by dissolving 1.2 g of L (+)-ascorbic acid (A15613, CAS50-81-7, Alfa Aesar) in 40 mL of DI water, and then 1.2 g of solid of ultrapure sodium dodecyl sulfate (J75819-22, CAS151-21-3, Thermo Scientific) was added into this 3% ascorbic acid solution. Note that it is recommended to prepare this solution 30 min before use, in order to stabilize its reducing strength, as otherwise, the slope of calibration line with freshly prepared reagent will be up to 5% steeper than those obtained later. Alternatively, to prevent loss of reducing strength, the solution should be deareated after preparation.

The oxalic acid solution was prepared by dissolving 0.8 g of oxalic acid anhydrous, ≥99.0% (75688-50G, CAS144-62-7, Sigma-Aldrich) in 40 mL of DI water. The solution was prepared daily.

3. Results and discussion

3.1. Optimization of the flow-batch assay protocol using a dye

To reproduce batch type conditions, the light path of a flow cell must be filled entirely with a stationary solution of uniform composition. Therefore, the leading and trailing edges of the sample zone which are diluted by the carrier solution on the way into the flow cell, must be situated outside the flow cell during the stop-flow measurement, as explained in section 1.1.2 and visualized in Fig. 3 step 3. This is achieved by using the software protocol (Fig. 4 step 2), where the volume of the diluted sample is set to 600 μL, and the transport volume TRv is set to 300 μL. This positions the centroid of the reaction mixture into the middle of the light path and leaves the leading and trailing edges outside the flow cell light path. The recording of absorbance (Fig. 5), obtained by monitoring the flow of a dye sample (BTB) in the flow cell, during the three stages of the protocol, shows the baseline (BS), recorded when the

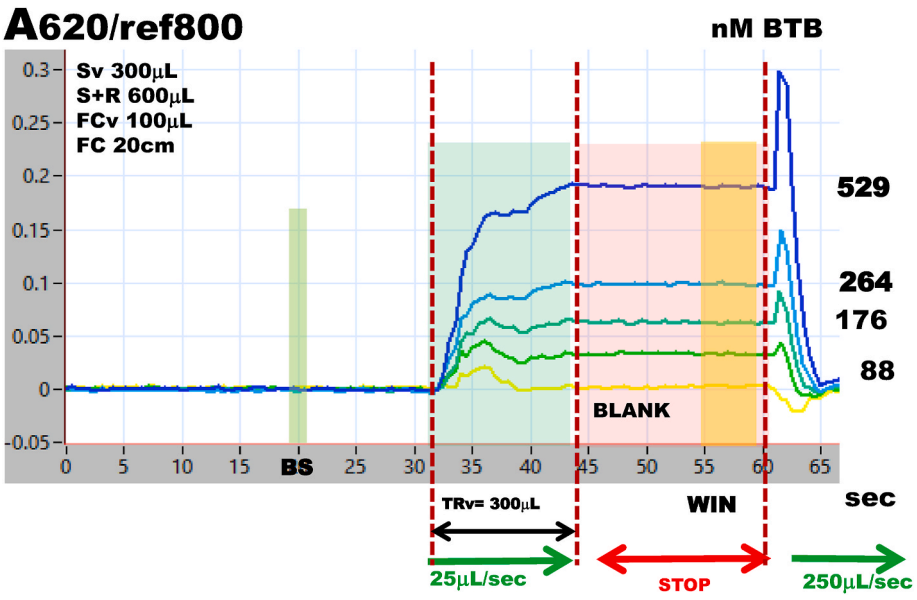

Fig. 5. Changes of absorbance recorded while standards of bromothymol blue (BTB), controlled by protocol Fig. 4, are passing through 20 cm long LLP cell. TRv- transfer volume, BS zero absorbance reading for baseline subtraction, WIN- absorbance collection interval. (For details see text). (For interpretation of the references to colour in this figure legend, the reader is referred to the Web version of this article.)

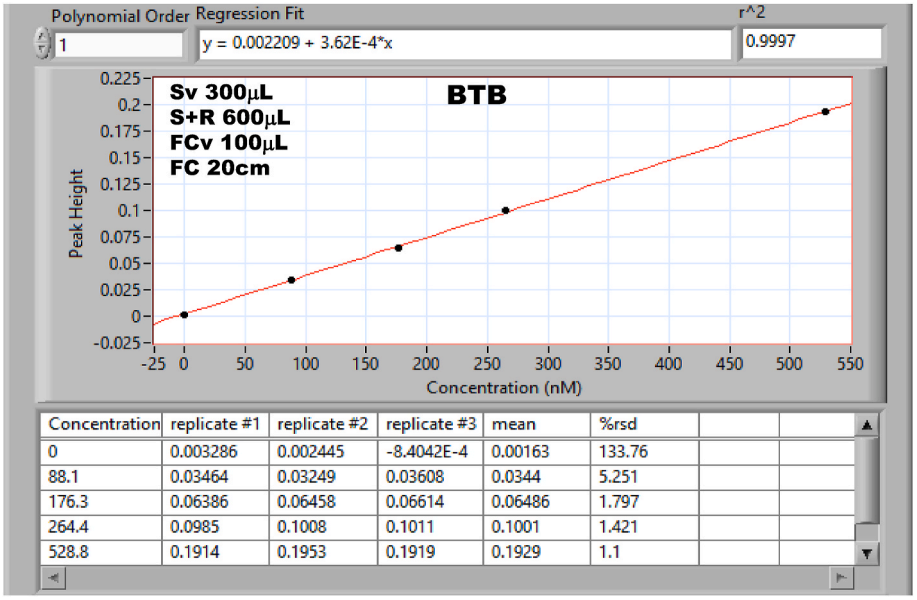

Concentration	replicate #1	replicate #2	replicate #3	mean	%rsd
0	0.003286	0.002445	-8.4042E-4	0.00163	133.76
88.1	0.03464	0.03249	0.03608	0.0344	5.251
176.3	0.06386	0.06458	0.06614	0.06486	1.797
264.4	0.0985	0.1008	0.1011	0.1001	1.421
528.8	0.1914	0.1953	0.1919	0.1929	1.1

Fig. 6. Calibration graph obtained by measuring standard solutions of bromothymol blue (BTB) and by plotting maximum absorbance recorded within data collection interval WIN Fig. 5. (For interpretation of the references to colour in this figure legend, the reader is referred to the Web version of this article.)

flow cell is filled with DI water, followed by a rise of the absorbance during sample transport into the flow cell. The absorbance monitoring period (WIN) is positioned at the end of stop-flow period when the absorbance readout has stabilized. The slope of the calibration line, obtained by the absorbance measurement within the WIN period, is 0.36 mAU/nM of BTB (Fig. 6) which when corrected for a sample and reagent (buffer) solution of S+R=1+1 dilution (step 2. Fig. 4) yields, in a 20 cm long flow cell, an absorptivity of 0.036 mAU/cm for 1 nM BTB.

Thus, 1 M BTB solution (m.w. 624) in 1 cm flow cell has absorbance $A = 3.63x10^4$ while according to the literature, the molar absorptivity of bromothymol blue at 620 nm: $\varepsilon = 3.57x10^4$ [20]. The agreement of these molar absorptivities confirms that this flow-batch technique operates as an equivalent to a traditional batch technique.

3.2. Nitrite assay

Determination of nitrite, based on the Gries reaction is the most frequently used assay for this analyte in sea water [21–23]. This chromogenic reaction produces an azo dye, which is pink in its protonated form ($\varepsilon = 4.6x10^4$ at 550 nm) [22,23]. In our previous work [12], we optimized the composition of the reagents and replaced phosphoric acid with sulfuric acid in the Gries reagent (section 2.2.3.), to avoid the potential of cross-contamination should the same instrument be used for a subsequent determination of traces of phosphate.

Since the determination of nitrite is a single reagent assay, it can be based on the flow scheme (Fig. 3) and assay protocol (Fig. 4) used for the BTB experiment, while using DI water as a carrier solution and the Gries reagent in port #3 on LOV. The absorbance/time graph (Fig. 7), obtained by analyzing nitrite standards (0–1.8 µM) comprises two sections: the flow

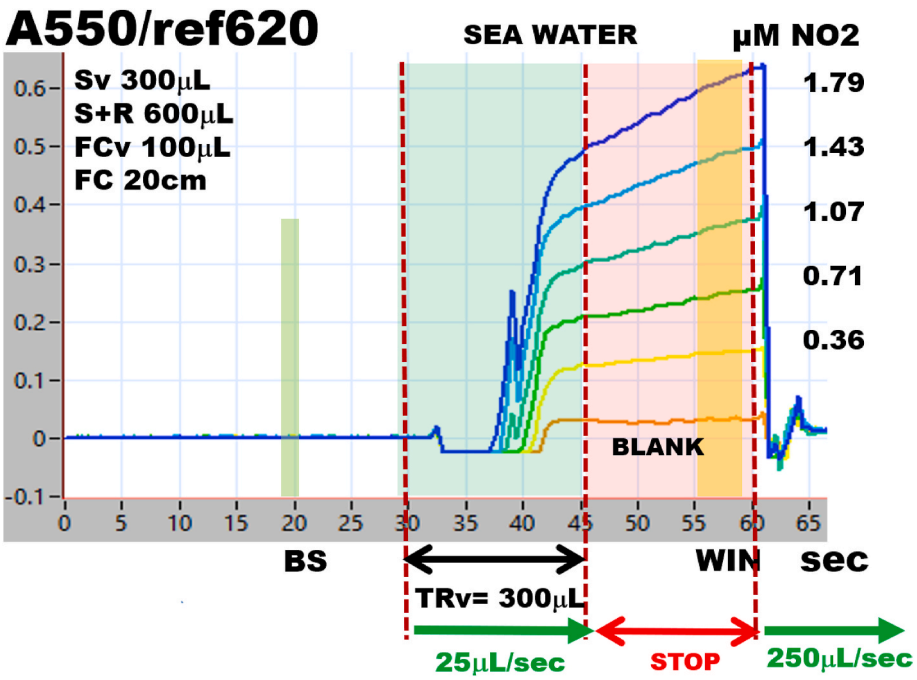

Fig. 7. Absorbance graph obtained with protocol Fig. 4., for analysis of nitrite standard solutions, prepared in sea water. BS – zero absorbance reading measured at this baseline, WIN - the highest absorbance measured within this window was used to construct calibration graph (Fig. 8.).

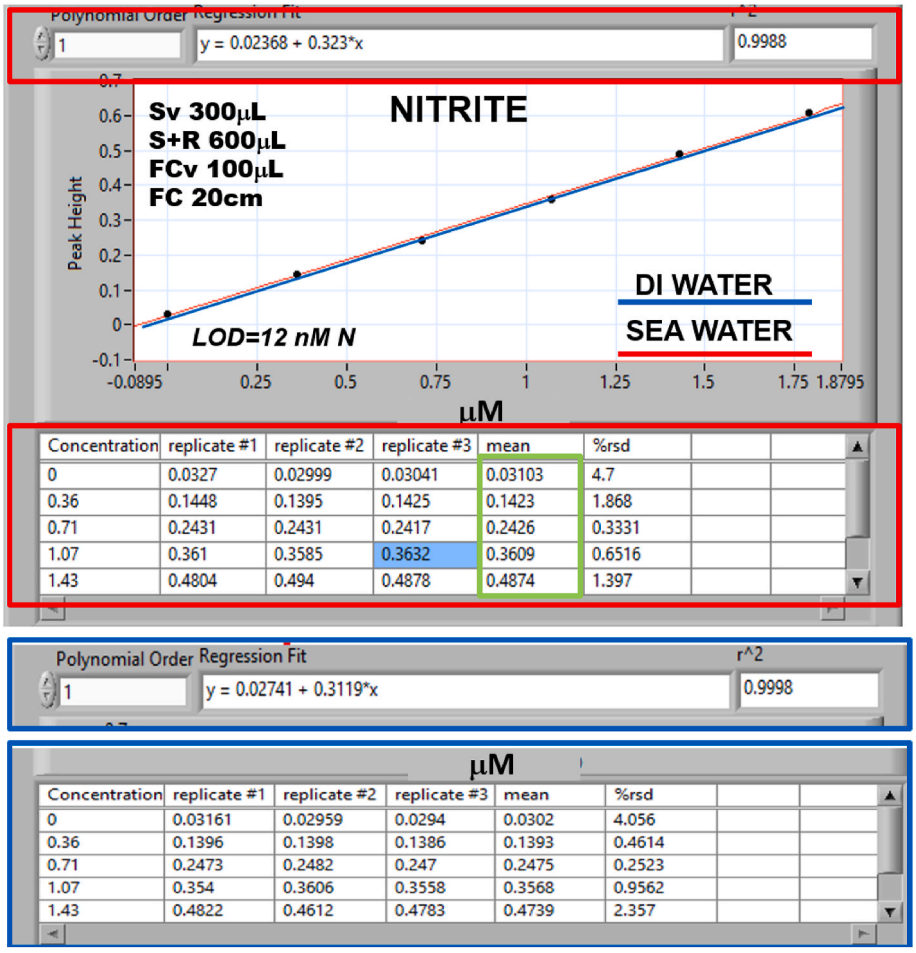

Fig. 8. Calibration data and calibration graph obtained by measuring standard solutions, of nitrite in DI water and in sea water, and by plotting maximum absorbance recorded within data collection interval WIN. Absorptivities in green box were used to calculate concentrations of nitrite in Table 1B. (For interpretation of the references to colour in this figure legend, the reader is referred to the Web version of this article.)

part up to 45 s, and the following stop-flow period lasting 15 s (shaded red). Changes of absorbance in the time interval shaded in green, recorded while the leading edge of the sample/reagent mixture enters the flow cell, depict the increasing concentration of the azo dye upon which the spikes, caused by the Schlieren effect are superimposed. Changes of the absorbance in the time interval shaded in red, while the reaction mixture is arrested within the flow cell, are due to an increasing concentration of the azo dye as the reaction proceeds. Absorbance values used to construct the calibration graph were collected towards the end of the stop-flow period (WIN), the sample/reagent mixing ratio S+R=1+1 (Fig. 3) is selected to extend the upper limit of the calibration range to 1 μM N.

However, as shown in our previous work [12], the sensitivity of the present variant (slope 0.312 AU/μM N, Limit of Detection (LOD)= 12 nM N in DI, Fig. 8.), can be increased by changing the sample/reagent mixing ratio to S+R=3+1 and by using 2.5 times longer light path (slope 1.04 AU/μM N, LOD= 0.6 nM N [12]).

Slopes and offsets of calibration lines as well as absorbance values (Fig. 8), obtained with standards prepared in DI water or SW are correlated well (Table 1) and discussed in section 3.6.

3.3. Nitrate assay

The Gries reaction is also used for the determination of nitrate, following its reduction to nitrite [19,21,23]. Despite an extensive search for alternative approaches [21], the reduction of the nitrate on a Cd/Cu column remains the most frequently used technique applied to sea water analysis, and therefore, we selected it for this study. To perform this assay successfully two conditions must be fulfilled: reduction must be carried out in a slightly alkaline buffer, and the column must not be exposed to air since oxygen deactivates its reducing power [19]. Therefore, the Cd column must be kept at all times filled with the alkaline buffer. This requirement is met by using an ammonium chloride buffer as a carrier solution in HC2 and by appropriate flow programming by P2 (Figs. 9 and 10). Since the Gries reaction must be carried out in an acid solution, the buffering capacity of the alkaline buffer and the acidity of the Gries reagent must be carefully balanced to allow the formation of the azo dye in the acid medium. The critical component of the experimental setup is the column (Fig. 2) filled with the granulated cadmium because its performance is determined by many variables; column length, diameter, particle size, packing, void volume, and flow rate [19]. These parameters, along with applied sample volume, determine the yield of the nitrate to nitrite conversion during contact with the reducing surfaces. Because the reduction of nitrate is very fast, it is feasible to use a short column with a void volume much smaller than the processed sample volume, and to achieve complete conversion under flowthrough conditions [24, Fig D]. Because aspiration of the sample from HC3 back through the Cd column into HC1 yielded irreproducible results, we used a bypass to return the sample via port 5 into LOV, in a similar way that Grand et al. used for sorbent extraction [25]. The addition of the Gries reagent (S+R= 3+1) dilutes the sample and extends the calibration range to 5 μM N (0.0831 AU/μM N, LOD = 94 nM N, in DI, Figs. 11 and 12). Slopes and offsets of calibration lines as well as absorbance values (Fig. 12), obtained with standards prepared in DI water or SW are correlated well (Table 1) and discussed in section 3.6.

3.4. Phosphate assay

Determination of phosphate, based on spectrophotometry of the

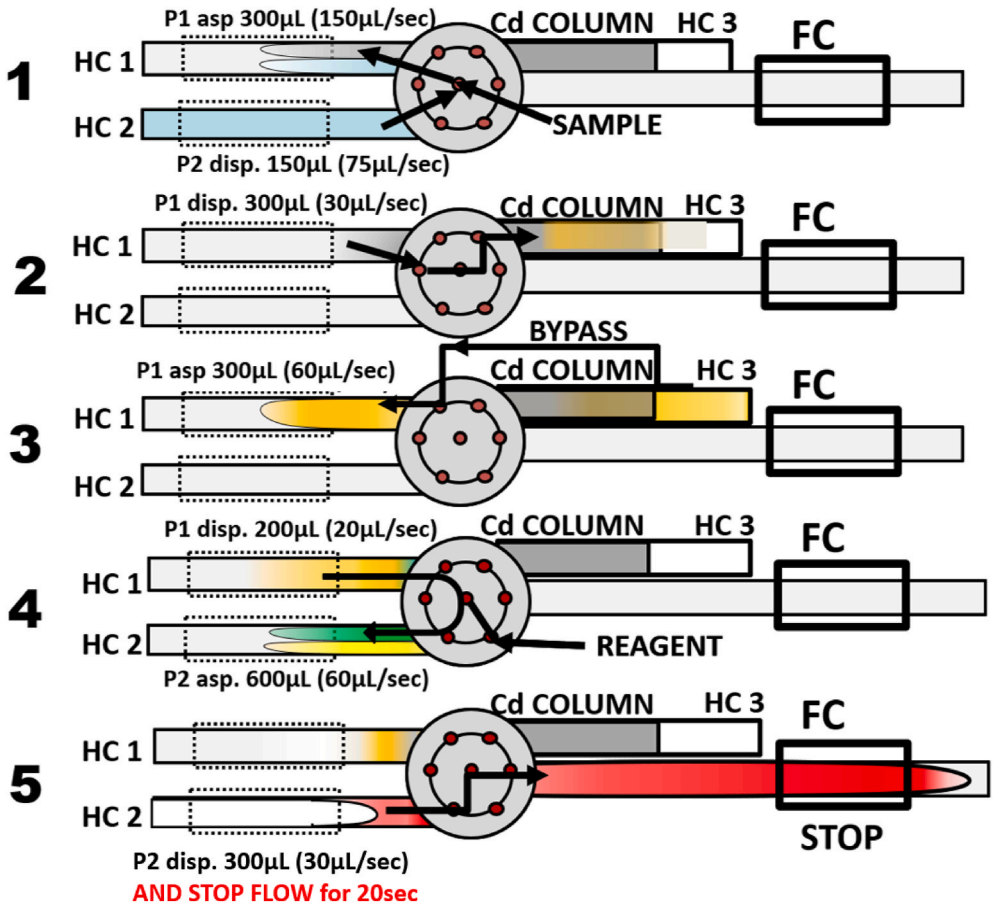

Fig. 9. Flow sequence for batch-flow assay of nitrate. The steps correspond to steps of assay protocol Fig. 10. Note bypass on step 3. FC- flow cell, HC1, HC2, HC3 - holding coils.

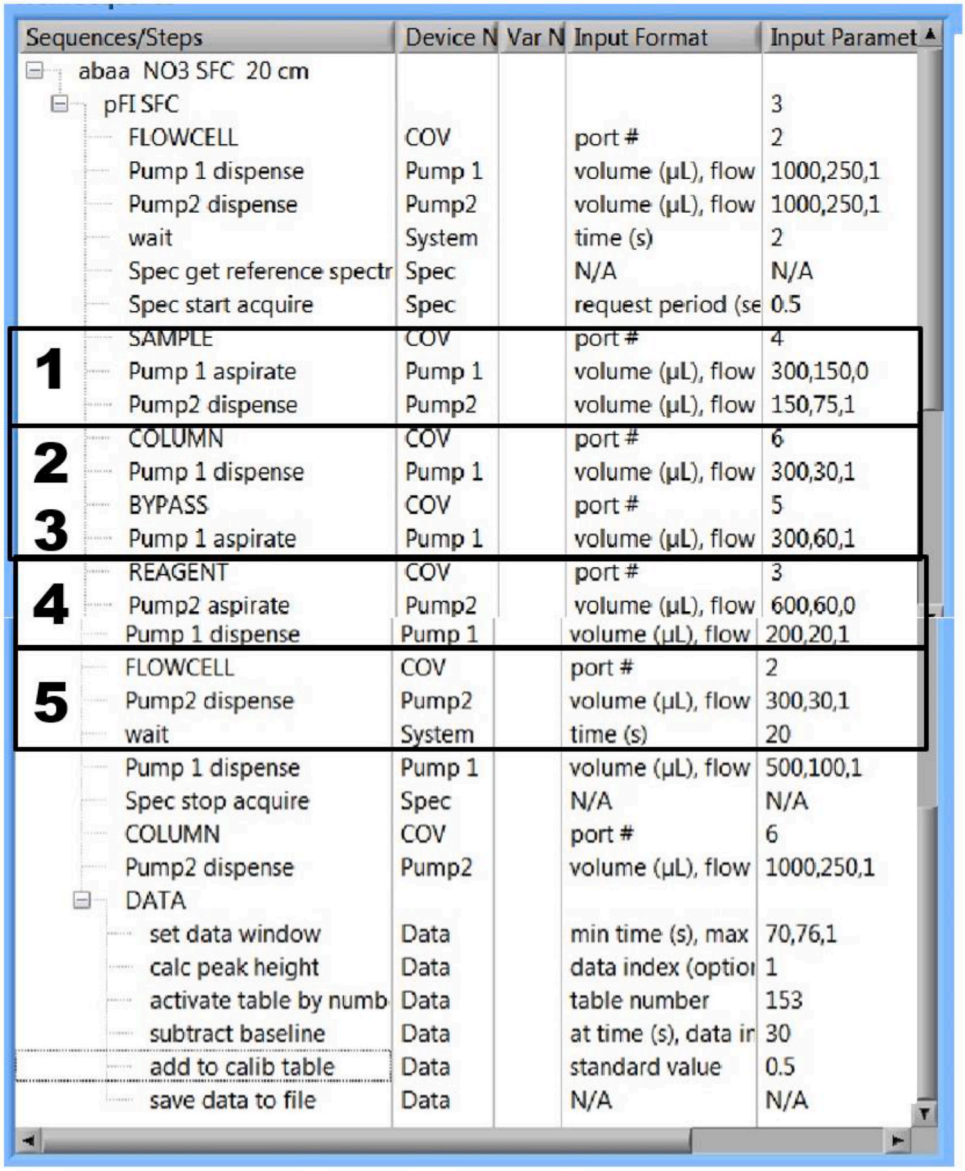

	Sequences/Steps	Device N	Var N	Input Format	Input Paramet
	abaa NO3 SFC 20 cm				
	pFI SFC				3
	FLOWCELL	COV		port #	2
	Pump 1 dispense	Pump 1		volume (µL), flow	1000,250,1
	Pump2 dispense	Pump2		volume (µL), flow	1000,250,1
	wait	System		time (s)	2
	Spec get reference spectr	Spec		N/A	N/A
	Spec start acquire	Spec		request period (se	0.5
1	SAMPLE	COV		port #	4
1	Pump 1 aspirate	Pump 1		volume (µL), flow	300,150,0
1	Pump2 dispense	Pump2		volume (µL), flow	150,75,1
2	COLUMN	COV		port #	6
2	Pump 1 dispense	Pump 1		volume (µL), flow	300,30,1
3	BYPASS	COV		port #	5
3	Pump 1 aspirate	Pump 1		volume (µL), flow	300,60,1
4	REAGENT	COV		port #	3
4	Pump2 aspirate	Pump2		volume (µL), flow	600,60,0
4	Pump 1 dispense	Pump 1		volume (µL), flow	200,20,1
5	FLOWCELL	COV		port #	2
5	Pump2 dispense	Pump2		volume (µL), flow	300,30,1
5	wait	System		time (s)	20
	Pump 1 dispense	Pump 1		volume (µL), flow	500,100,1
	Spec stop acquire	Spec		N/A	N/A
	COLUMN	COV		port #	6
	Pump2 dispense	Pump2		volume (µL), flow	1000,250,1
	DATA				
	set data window	Data		min time (s), max	70,76,1
	calc peak height	Data		data index (optio	1
	activate table by numb	Data		table number	153
	subtract baseline	Data		at time (s), data ir	30
	add to calib table	Data		standard value	0.5
	save data to file	Data		N/A	N/A

Fig. 10. Assay protocol for batch-flow assay of nitrate. The steps correspond to steps in the flow sequence Fig. 9.

phosphomolybdenum blue (PMoB), has been widely used for the determination of this analyte in sea water [6,21]. The PMoB is produced in two steps; first yellow phosphomolybdate (PMo) is rapidly formed, followed by the gradual formation of the PMoB compound upon addition of a reducing agent. Both reactions are performed in a strongly acid solution (pH 0–1) to prevent interference from molybdenum blue (MoB) as well as from silica molybdenum blue (SiMoB), which is formed in the presence of silicic acid. A variety of reducing agents have been proposed in the perpetual quest for the optimization of the PMoB method [26], ascorbic acid being preferred in oceanographic applications [6,21,27]. The acidity of the molybdate reagent (section 2.2.4.) is critical since too low an acidity results in the formation of colloidal molybdenum that coats the flow cell and manifold and increases the absorbance readout over the entire wavelength range. It is therefore recommended to adjust the acidity of the molybdate reagent so that the spectrum in the presence of phosphate is as shown in [28, Fig. C]. The assay protocol (Figs. 13 and 14) used here, is based on our previous investigation of the optimized condition for the determination of phosphate by pFI [18], the adjustment of the sample and reagent volumes in this work is being made to fulfill the requirements of the flow-batch method (Fig. 14 step 4).

The absorbance/time graph (Fig. 15), obtained by analyzing phosphate standards (0–3.0 µM) comprises two sections: the flow part up to 62 s and the following stop-flow period lasting 40 s (shaded red). Changes of absorbance, monitored at 880 nm, within the time interval shaded in green, are recorded while the leading edge of the sample/reagent mixture enters the flow cell, depicted by the increasing concentration of PMoB superimposed on an initial dip, caused by the Schlieren effect. Absorbance values were collected at the end of the stop-flow period (WIN). Dilution of the sample with the mixed reagents (S+R= 3+1) yields a slope of 0.136 AU/µM P, LOD = 47 nM P in DI (Fig. 16). Under these conditions, the phosphate determination is not influenced by the presence of a large excess of silicate as shown in Fig. 15, where addition of 340 µM Si (>2x the highest seawater values) did not elevate the blank value. Slopes and offsets of calibration lines as well as absorbance values (Fig. 16), obtained with standards prepared in DI water or SW are correlated in Table 1 and discussed in section 3.6.

3.5. Silicate assay

Determination of silicate-based on the spectrophotometry of the

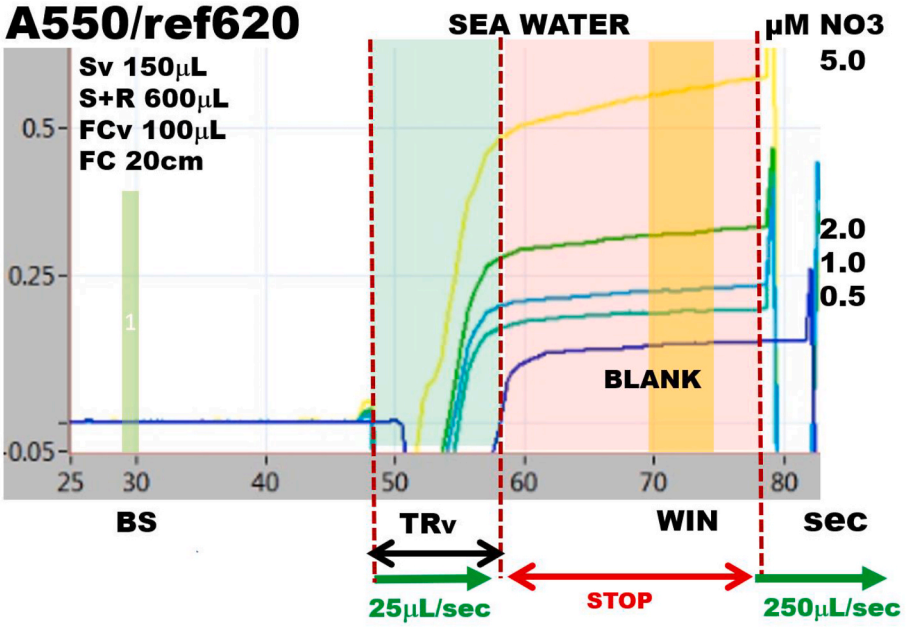

Fig. 11. Absorbance graph obtained with protocol Fig. 10., for analysis of nitrate standard solutions, prepared in sea water. BS – zero absorbance reading measured at this baseline, WIN - the highest absorbance measured within this window was used to construct calibration graph (Fig. 12.) TRv-transport volume.

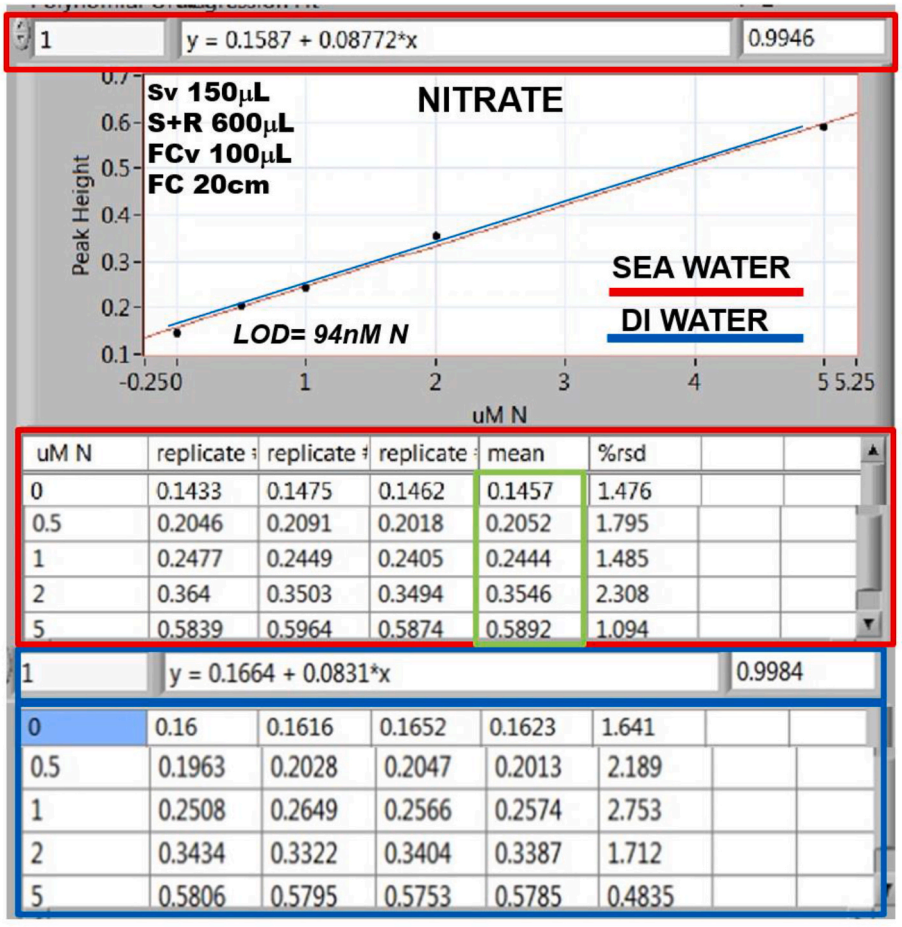

Fig. 12. Calibration data and calibration graph obtained by measuring standard solutions, of nitrate in DI water and in sea water, and by plotting maximum absorbance recorded within data collection interval WIN. Absorptivities in green box were used to calculate concentrations of nitrate in Table 1B. (For interpretation of the references to colour in this figure legend, the reader is referred to the Web version of this article.)

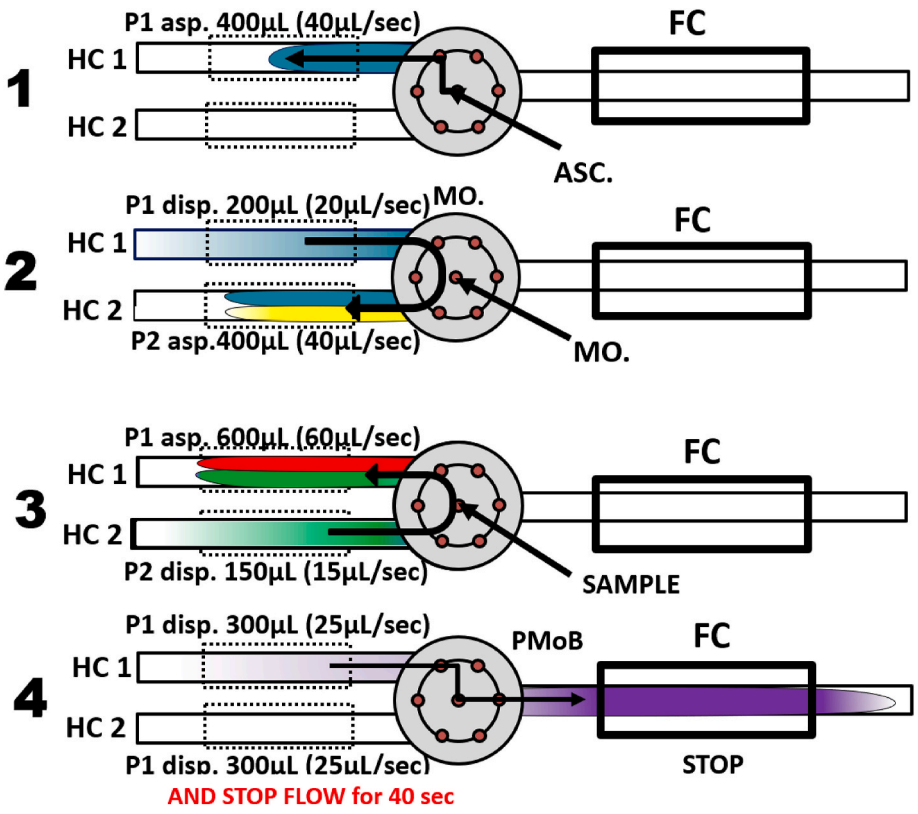

Fig. 13. Flow sequence for batch-flow assay of phosphate. The steps correspond to steps of assay protocol Fig. 14. FC- flow cell, HC1, HC2 - holding coils.

Work Sequence

	Sequences/Steps	Device N	Var Name	Input Format	Input Parameters
	FLOWCELL	COV		port #	2
	Pump1 dispense	Pump1		volume (µL), flow rate	1000,250,1
	Pump2 dispense	Pump2		volume (µL), flow rate	1000,250,1
	wait	System		time (s)	10
	Spectrometer get referen	Spectror		N/A	N/A
	Spectrometer start acquir	Spectror		request period (secon	0.5
1	ASCORBIC ACID	COV		port #	5
	Pump1 aspirate	Pump1		volume (µL), flow rate	400,40,1
2	MOLYBDATE	COV		port #	3
	Pump2 aspirate	Pump2		volume (µL), flow rate	400,40,0
	Pump1 dispense	Pump1		volume (µL), flow rate	200,20,1
	wait	System		time (s)	2
3	SAMPLE	COV		port #	4
	Pump1 aspirate	Pump1		volume (µL), flow rate	600,60,0
	Pump2 dispense	Pump2		volume (µL), flow rate	150,15,1
4	FLOWCELL	COV		port #	2
	Pump1 dispense	Pump1		volume (µL), flow rate	300,25,1
	wait	System		time (s)	40
	Pump2 dispense	Pump2		volume (µL), flow rate	2000,250,1
	Pump1 dispense	Pump1		volume (µL), flow rate	2000,250,1
	Spectrometer stop acquir	Spectror		N/A	N/A
	subtract baseline	Data		at time (s), data index	10
	set data window	Data		min time (s), max tim	99,102

Fig. 14. Assay protocol for batch-flow assay of phosphate. The steps correspond to steps in the flow sequence Fig. 13.

silicomolybdenum blue (SiMoB) is a three-reagent assay.

First, the silicomolybdate (SiMo) is formed in a mildly acid medium, where, if phosphate is present, phosphomolybdate (PMo) is also formed. To avoid phosphate interference oxalate is added in the second step to decompose PMo [29–31]. We used ascorbic acid to reduce SiMo to SiMoB and performed the entire reagent sequence at an elevated temperature while the reaction mixture was being held during the stop flow periods in the thermostated holding coils at 50 °C (Figs. 17 and 18). Finally, the reaction mixture was transported into the flow cell where the absorbance was monitored for a 30 s stop flow period. The composition of the reagents is detailed in section 2.2.5.

The absorbance/time graph (Fig. 19), obtained by analyzing silicate standards (0–27 µM) comprises two sections: the flow part up to 110 s and the following stop-flow period lasting 30 s (shaded red). Changes of

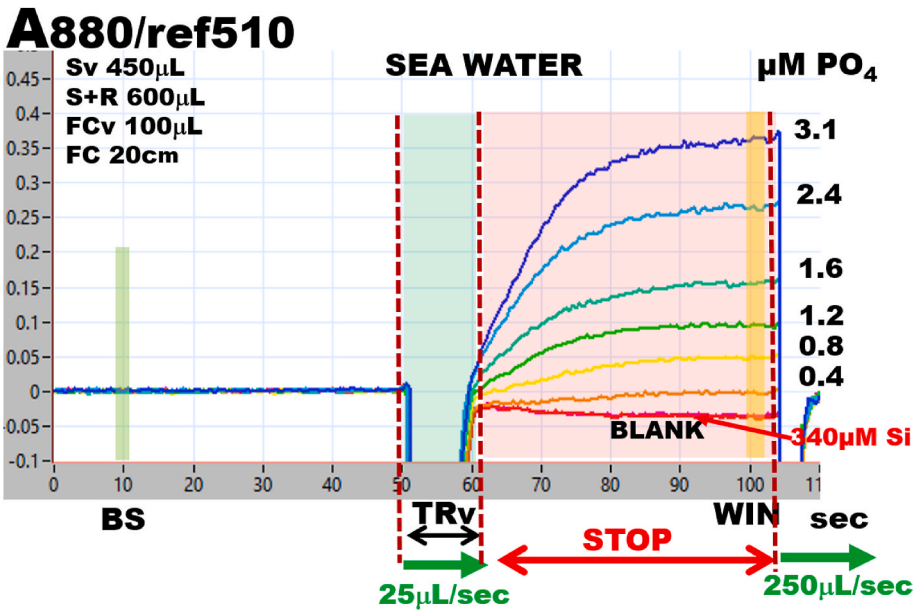

Fig. 15. Absorbance graph obtained with protocol Fig. 14., for analysis of phosphate standard solutions, prepared in sea water. BS – zero absorbance reading measured at this baseline, WIN - the highest absorbance measured within this window was used to construct calibration graph (Fig. 16.) TRv-transport volume.

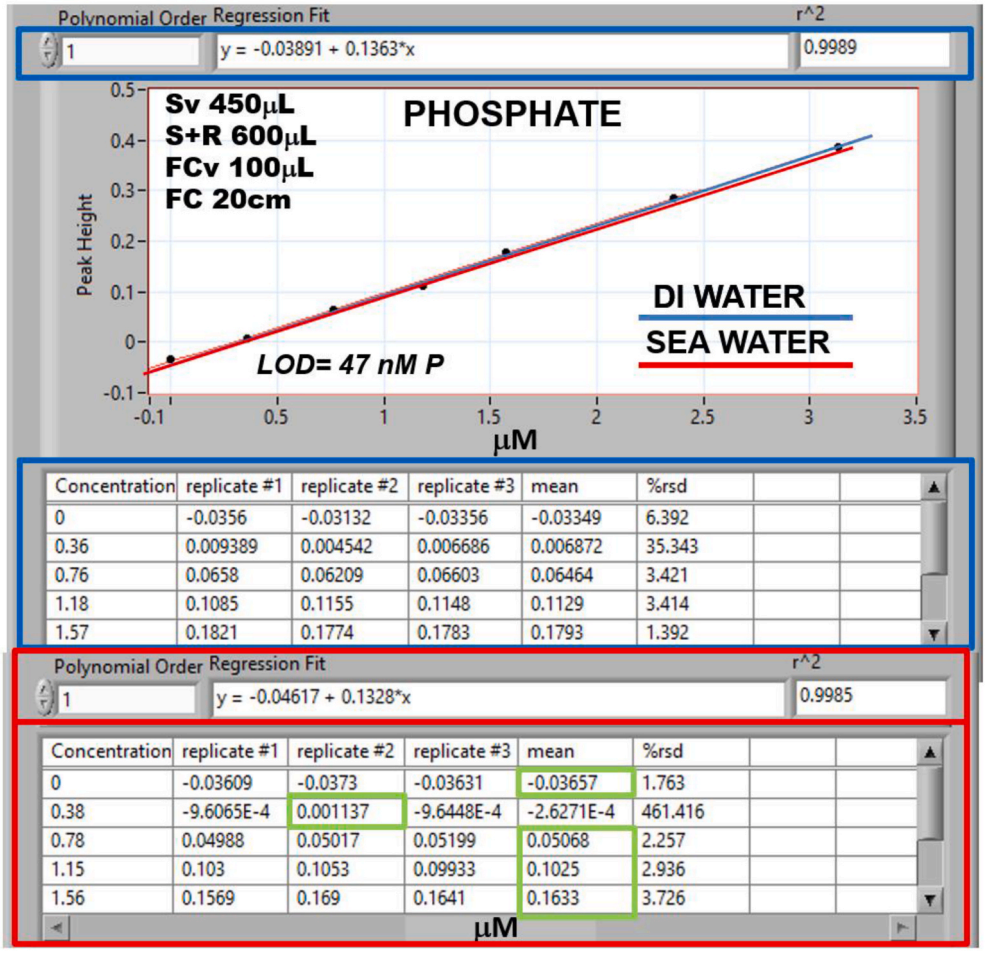

Concentration	replicate #1	replicate #2	replicate #3	mean	%rsd
0	-0.0356	-0.03132	-0.03356	-0.03349	6.392
0.36	0.009389	0.004542	0.006686	0.006872	35.343
0.76	0.0658	0.06209	0.06603	0.06464	3.421
1.18	0.1085	0.1155	0.1148	0.1129	3.414
1.57	0.1821	0.1774	0.1783	0.1793	1.392

Concentration	replicate #1	replicate #2	replicate #3	mean	%rsd
0	-0.03609	-0.0373	-0.03631	-0.03657	1.763
0.38	-9.6065E-4	0.001137	-9.6448E-4	-2.6271E-4	461.416
0.78	0.04988	0.05017	0.05199	0.05068	2.257
1.15	0.103	0.1053	0.09933	0.1025	2.936
1.56	0.1569	0.169	0.1641	0.1633	3.726

Fig. 16. Calibration data and calibration graph obtained by measuring standard solutions, of phosphate in DI water and in sea water, and by plotting maximum absorbance recorded within data collection interval WIN. Absorptivities in green box were used to calculate concentrations of phosphate in Table 1B. (For interpretation of the references to colour in this figure legend, the reader is referred to the Web version of this article.)

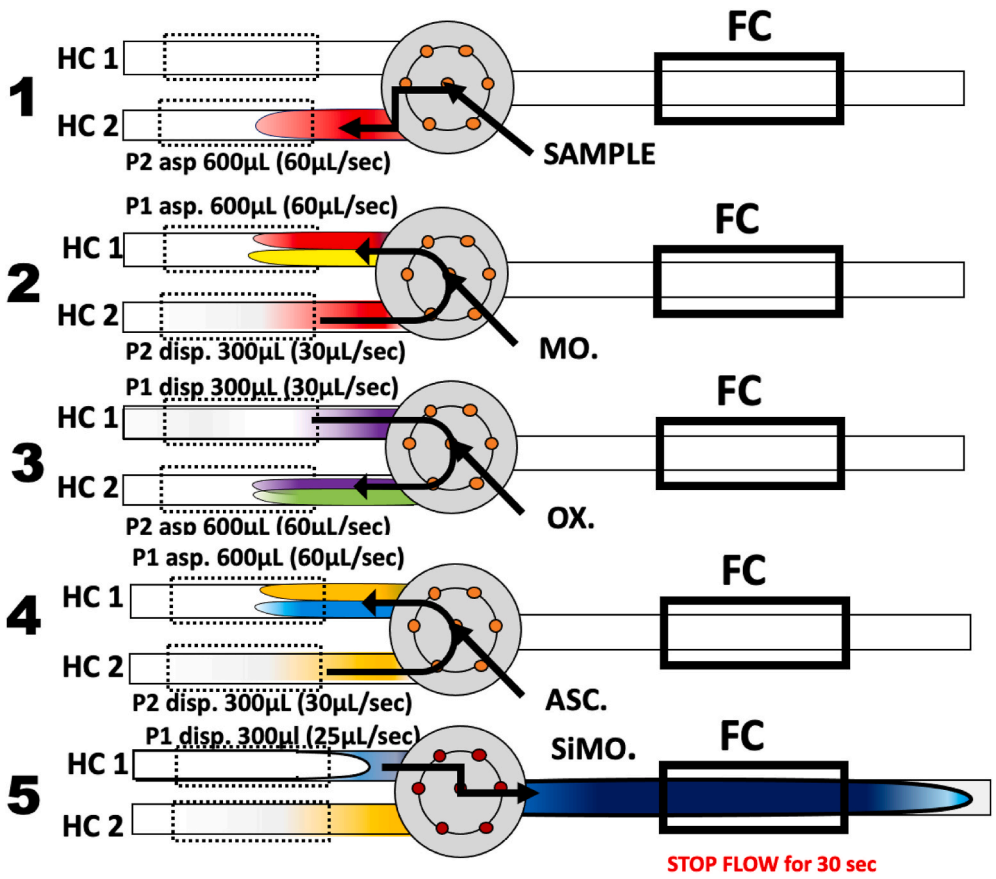

Fig. 17. Flow sequence for batch-flow assay of silicate. The steps correspond to steps of assay protocol Fig. 18. FC- flow cell, HC1, HC2 – holding coils.

absorbance, monitored at 810 nm, within the time interval shaded in green, are recorded while the leading edge of the sample/reagent mixture enters the flow cell. They depict the increasing concentration of SiMoB superimposed on a dip, caused by the Schlieren effect. Steady-state absorbance during the time interval shaded in red indicates that the formation of SiMoB has reached equilibrium. Calibration graphs (Fig. 20) were constructed from absorbance values collected towards the end of the stop-flow period (WIN, Fig. 19.). During the five-step protocol, the sample is sequentially diluted with various reagents (Figs. 17 and 18). In step 2, S+R= 1+1, in step 3, S+R=1+1, and in step 4, S+R= 1+1 resulting in a 8x dilution of the initial sample concentration. This results in an upper limit of the calibration range of 30 µM (slope 0.037 AU/µM Si, LOD= 240 nM in DI, Fig. 20.). The presence of phosphate (4.1 µM P) did not elevate the blank value (Fig. 19.), and since the phosphate concentration in open sea water does not exceed 3 µM P, the silica determination is free from phosphate interference. Slopes and offsets of calibration lines as well as absorbance values (Fig. 20.), obtained with standards prepared in DI water or SW are correlated in Table 1 and discussed in section 3.6.

3.6. *Correlation of calibrations obtained with standards prepared in DI and sea water*

Results, presented in the previous section document that the Schlieren effect is eliminated by measuring the absorbance of a stationary homogenous solution arrested in the flow cell (WIN, Figs. 7, 11, 15 and 19). As a result, the precision of the absorbance measurements for nutrient determinations in this work is on average 3% rsd.

However, to establish that DI standards can be used to analyze sea water samples, the calibration responses must be linear (Figs. 8, 12, 16 and 20). And the slopes and the offsets of calibration lines, obtained with standards prepared in DI and SW, should be identical, or be close enough to result in an error of determination of no more than 3%.

When the *slopes* of the calibration lines, defined by the Calibration Ratio, CR = X_{DI}/X_{SW}= 1.000, confirms that chemical reactions in DI and SW are proceeding at the same rate, and thus producing the same concentration of monitored species. For phosphate and silicate, those ratios at 1.026, and 1.033 are within the 3% error of the method. However, in the case of nitrite and nitrate, (Table 1. A, column 4), it can be seen that the X_{DI}/X_{SW} are 0.966 and 0.948, and therefore the CR value should be used to accommodate the difference in reaction rates in DI and SW.

While this ratio of the slopes is most reliably measured when the reaction has reached equilibrium, (Figs. 15 and 19), a CR value obtained at incomplete reaction such as nitrite (Fig. 7.) can also be applied to obtain correct results (Table 1B). It is important to note that the ratio of the slopes will be influenced by any changes of temperature or of the specific reaction conditions.

The *offset,* the second variable of the linear regression ranges in this work from −38.9 mAU to 166.4 mAU in the DI calibration (Table 1A, column 2). To understand this offset, the nitrite assay was performed by using DI water as carrier, under the same conditions as in Figs. 7 and 8, albeit at a concentration, close to the LOD. The absorbance/time recording lines (Fig. 21) of standards in DI and sea water (BLANK 1 & 2) and of 150 nM N (spiked in DI water) were obtained using the Gries reagent. Two additional absorbance/timelines were obtained using a DI water sample (dark blue line) and a SW sample (light blue line) where the Gries reagent had been replaced by DI water, meaning that no reagent was added. Additionally, the absorbance of the LOD = 17 nM N is indicated with a dashed line on this figure. Note that all lines share the same baseline, which was recorded while the flow cell was filled with a stationary carrier – DI water, and the absorbance value of the baseline was set to zero at BS time. Notice that, the dark blue line of the DI sample

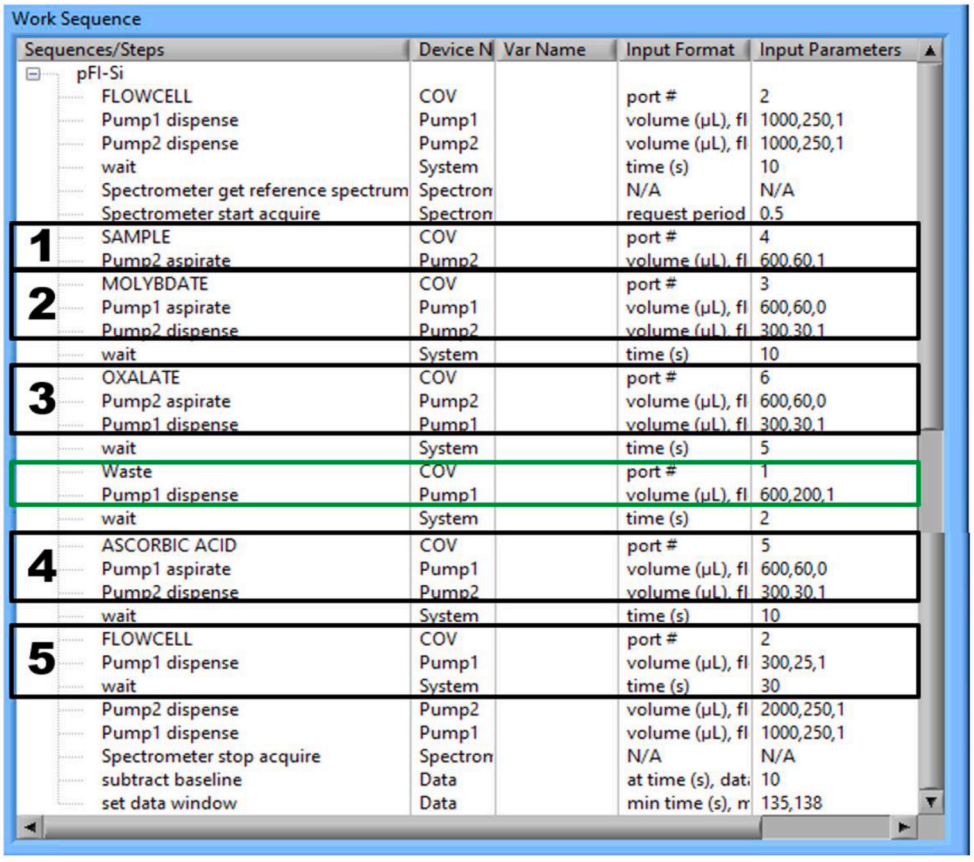

Fig. 18. Assay protocol for batch-flow assay of silicate. The steps correspond to steps in flow sequence Fig. 17, which, however does not include wash step (in green frame). (For interpretation of the references to colour in this figure legend, the reader is referred to the Web version of this article.)

continues, during the flow condition, at a slightly elevated level, reaching 7.3 mAU units above baseline at WIN. In contrast, the light blue line of the SW sample undergoes a large Schlieren dip, after which it returns almost to baseline level, ending at 3.8 mAU at WIN, which is below that of the DI sample. The difference between these values, 3.5 mAU is the matrix blank. Absorbance values at WIN of BLANK 1 (SW)= 30.2 mAU, and of BLANK 2 (DI)=30.6 mAU, (both containing all reagents) are much higher, which confirms that the reagent is the major component of the absorbance which is designated as the BLANK on the absorbance recordings (Figs. 5, 7, 11, 15 and 19).

Therefore, it is the not the BLANK value, but the *difference of BLANKS* between DI and SW that determines if the DI calibration is suitable for applying to SW samples. If this difference of BLANKS is zero or smaller than 3% of concentration of determined sample value, DI calibration is

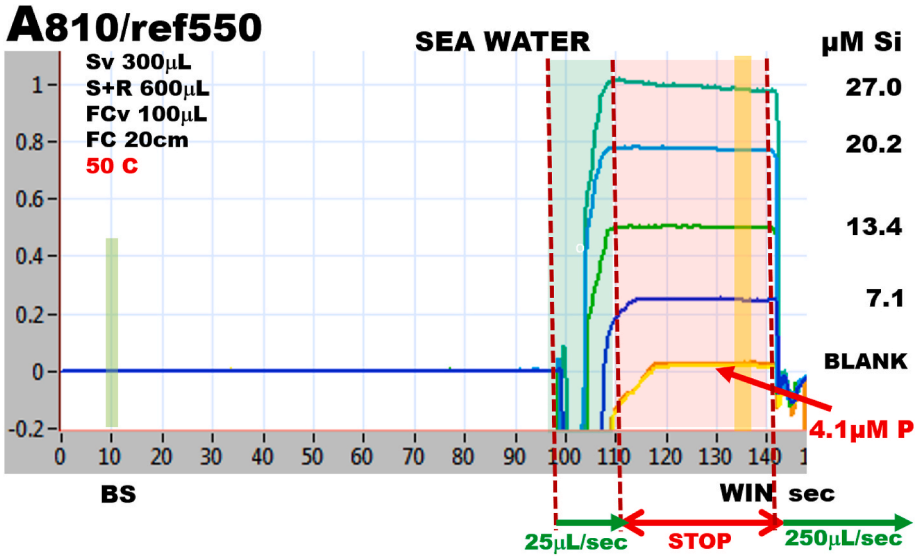

Fig. 19. Absorbance graph obtained with protocol Fig. 18., for analysis of silicate standard solutions, prepared in sea water. BS – zero absorbance reading measured at this baseline, WIN - the highest absorbance measured within this window was used to construct calibration graph (Fig. 20.) TRv-transport volume.

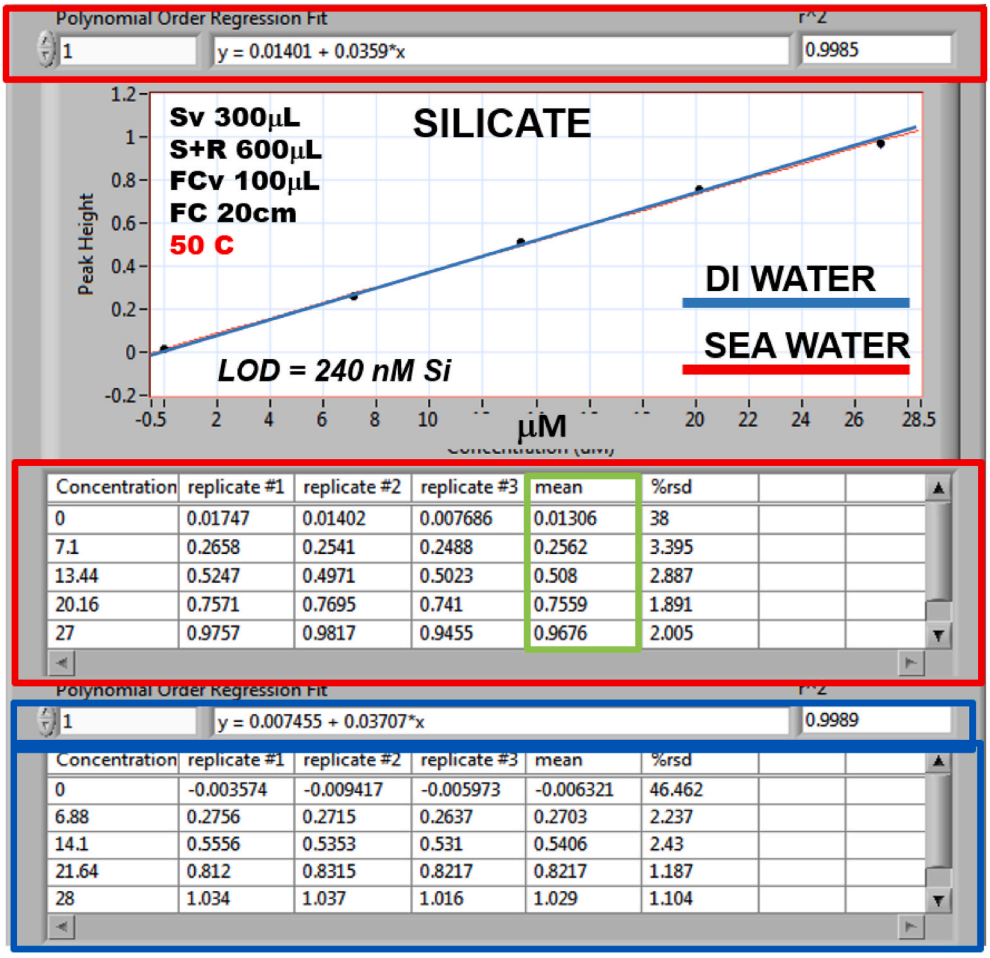

Fig. 20. Calibration data and calibration graph obtained by measuring standard solutions, of silicate prepared in DI water and in sea water, and by plotting maximum absorbance recorded within data collection interval WIN. Absorptivities in green box were used to calculate concentrations of silicate in Table 1B. (For interpretation of the references to colour in this figure legend, the reader is referred to the Web version of this article.)

suitable, otherwise the offset of DI calibration line has to be adjusted. Since BLANK values are related to offsets (O) of DI and SW calibration lines, it is the *difference in offsets* (OD) expressed in nM of the given analyte (Table 1 column 5) that can be used to calculate suitability of using a DI calibration for SW determinations. Therefore, it is the OD/LS value where LS is the concentration of Lowest Standard used to obtain calibration equation (Table 1A column 7), that can serve as a benchmark to determine when DI calibration equation will result the acceptable 3% error within the calibration range *above* LS value. This is because OD/LS ratio increases with decreasing concentration and therefore error due to DI calibration will be larger than 3% at sample concentrations below LS. Values of this benchmark concentration defined as OD/LS% are shown in Table 1B column 6. Therefore, the DI calibration equation can be used without modification for determination of nitrite, nitrate and silicate in SW samples situated within the concentration range above LS value. For determination of these analytes below LS value and for determination of phosphate, if the error of 15% at a P concentration of 360 nM P is not acceptable, the SW calibration equation must be used.

Another way to determine the error caused by the difference in the slopes and the offsets of the calibration equations is to investigate if the

Table 1
Correlation of calibration data and estimate of errors of determination.

A	DI Calibration	SW Calibration	CR = Xdi/Xsw	Offset DI-SW (OD, nM)	Lowest Standard (LS, nM)
NITRITE	Y = 0.0274 + 0.3119 X	Y = 0.02368 + 0.3230 X	0.966	12	360
NITRATE	Y = 0.1664 + 0.0831 X	Y = 0.1587 + 0.0877 X	0.948	93	500
PHOSPHATE	Y = −0.03891 + 0.1363 X	Y = −0.04617 + 0.1328 X	1.026	53	360
SILICATE	Y = 0.00746 + 0.0371 X	Y = 0.0140 + 0.0359 X	1.033	176	7100

B	DI x CR Calibration (µM)	SW Calibration (µM)	DR=DI/SW	Mean DR	OD/LS %
NITRITE	1.42, 1.03, 0.67, 0,36, 0.01	1.44, 1.04, 0.68, 0.37, 0.02	0.992, 0.989, 0.983, 0.969	0.984	3.3
NITRATE	4.82, 2.15, 0.89, 0.44, −0.24	4.91, 2.23, 0.98, 0.53, −0.15	0.983, 0.961, 0.911, 0.835	0.922	1.86
PHOSPHATE	1.56, 1.06, 0.67, 0.30, 0.02	1.58, 1.12, 0.73, 0.36, 0.07	0.965, 0.951, 0.925, 0.846	0.922	14.7
SILICATE	26.74, 20.85, 13.94, 6,93, 0.16	26.56, 20.67, 13.76, 6.75, −0.03	1.006, 1.008, 1.013, 1.027	1.014	2.48

A: calibration lines, slope ratio, and offset of intercepts of DI and SW standard solutions. B: calculated SW values using calibration lines. Note: DI-deionized water, SW-Open ocean surface water, CR-calibration ratio, OD-difference in offset values, LS- lowest standard value, DR-determination ratio. Concentrations in DI and SW in mM were calculated from absorptivity shown in green boxes, Figs. 8, 12, 16 and 20.

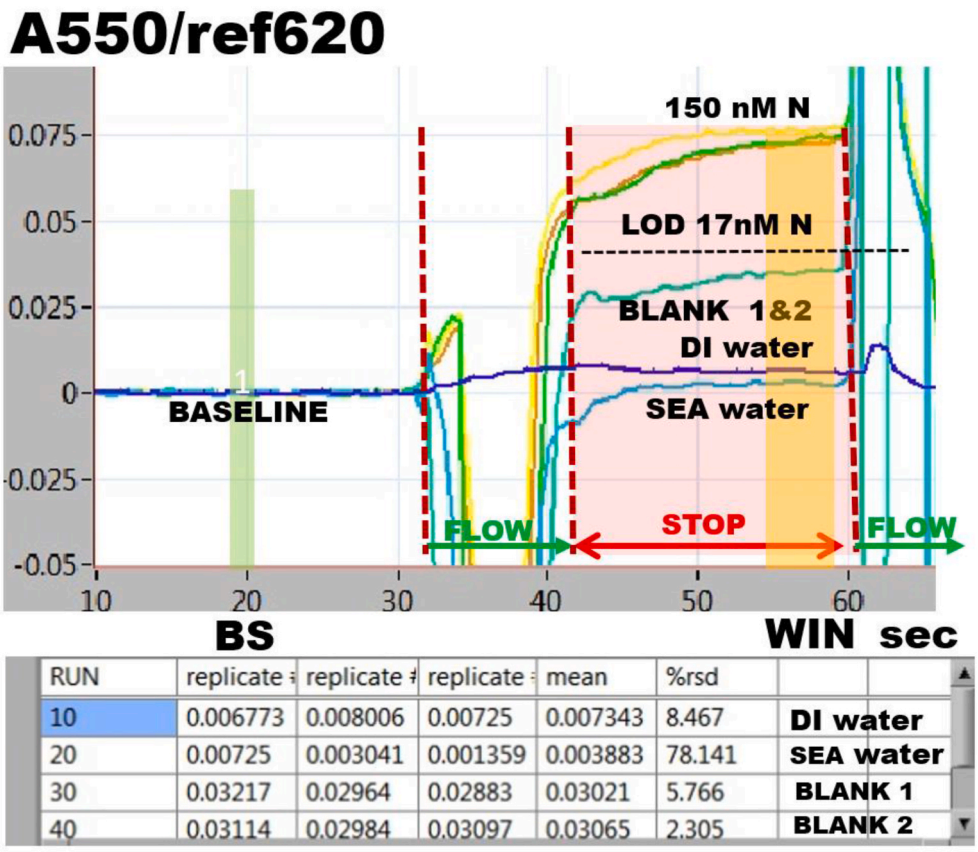

RUN	replicate	replicate	replicate	mean	%rsd	
10	0.006773	0.008006	0.00725	0.007343	8.467	DI water
20	0.00725	0.003041	0.001359	0.003883	78.141	SEA water
30	0.03217	0.02964	0.02883	0.03021	5.766	BLANK 1
40	0.03114	0.02984	0.03097	0.03065	2.305	BLANK 2

Fig. 21. Components of blank. Absorbance graph obtained with protocol Fig. 4. for analysis of nitrite using DI water as carrier. DI water – sample and reagent are DI water. SEA water-sample is SW reagent is DI water, BLANK 1&2, sample is SW or DI, and Gries reagent. Sample containing 150 nM N as nitrite was run three times. LOD was calculated from DI water blank value in data table. For details see text.

DI equation (Table 1A, column 2) multiplied by the Calibration Ratio (X_{DI}/X_{SW} = CR, Table 1A column 4) will yield the same result as the SW calibration equation (Table 1B, column 3), when used for the analysis of SW samples. This can be found by analyzing a set of standards prepared in SW by using DI and SW calibration equations (Table 1B columns 2 and 3) and by correlating the results obtained by calculating the Determination Ratio, DR = DI/SW (Table 1B, column 4). This was done by using the absorbance data obtained by analyzing SW or DI standards of nitrite, nitrate, phosphate, and silicate (Figs. 8, 12, 16 and 20, green frame). The results, summarized in Table 1B, column 5, show that the *means* of the calculated DR values (Table 1B, column 5), are within 3% of the corresponding CR values (Table 1A, column 4) and therefore the calibration equation obtained with DI water standards, when multiplied by CR value can be used for the determination of sea water samples. The exception are results for the phosphate calculation (Table 1B), where CR = 1.026 while DR = 0.922. By adjusting the offset of the DI calibration line by 53 nM P, the value of OD (Table 1A.), results in DR = 0.998.

In summary, the influence of Schlieren effect is completely eliminated by performing measurements in a batch mode. The difference in *reaction rates* in DI and SW matrix can be corrected by the calibration ratio (CR), but a large difference in *offsets* of calibration lines obtained in DI and SW calibrations, as is the case of phosphate determination (Table 1.), will result in unacceptable error. Inevitably, all calibration methods fail as the concentrations below the lowest calibration standard (LS) approach the limit of detection -and so it does with SLC. Whether this is because differences in offsets (OD) of nitrite, nitrate, phosphate, and silicate (Table 1A, column 5) are remarkably close to the LOD of these analytes (Figs. 8, 12, 16 and 20), and whether this is a limitation or a coincidence we will attempt to resolve, along with investigation of the factors that influence run to run and day to day variations of offsets and the slopes of the calibration lines.

3.7. *Implementation of Single Line Calibration technique*

When SLC is being implemented, it is recommended to verify the function of the instrument by performing the dye experiment (section 2.2.2.). The slope and offset of the calibration line should be within 10% of the values listed in Fig. 6 rsd = 3% or less, and r^2= 0.999. For application to nutrient assays use reagents and protocols described in section 2. First, calibrate the instrument using DI based standards. If the slopes and offset of the calibration line are within 10% of values in Table 1A, column 2, the DI x CR calibration can be used for analysis of SW samples. If the *slopes* are different from values shown in Table 1A, adjust reagents and conditions by following the information given in Section 3, next perform DI and SW calibrations and correlate the data as described in Section 3 and Table 1. If the value of OD/LS% is elevated, it may be due to a presence of analyte and/or high matrix of sea water used. To resolve this issue, run SW samples collected at different conditions and compare them, thus obtained BLANK absorbances with absorbance of DI water BLANK (Fig. 21.).

4. Conclusion

Programming of FI in batch flow mode eliminates the Schlieren effect and opens the door to implementation of Single Line Calibration technique, based on the correlation of calibration obtained with DI water-based standards with calibration obtained with sea water-based standards. This means that ultimately it may be no longer be necessary to use low nutrient sea water (LNSW) to produce calibration standards for use in oceanography, an advantage that will facilitate work in laboratories

that do not have ready access to this material and will eliminate the problems of storing it for those who can obtain it. However, while it is documented in this work that SLC is applicable to a variety of reagent-based assays, it was only used with sea water collected from a single location. Therefore, the usefulness of SLC still has to be confirmed by using sea water from several different locations with different levels of dissolved organic carbon and other micro components.

In contrast to all other flow-based techniques, pFI uses DI water as the carrier. This yields a well-defined baseline, that is reset at the beginning of *each measurement cycle.* This feature combined with calibration using DI based standards provides a reproducible framework for serial measurements and for laboratory intercomparisons. Furthermore, the high flow rate rinse with DI stream, eliminates baseline drift and carryover, a significant drawback of continuous flow FI, as well as of all air segmented continuous flow analyzers [32,33], that rely on using a reagent-based baseline, that changes with the reagent composition, and also causes continuous reagent consumption and waste generation.

For this work, we chose the frequently performed nutrient assays, based on a variety of reagents, to document the versatility of flow programming, which accommodates a variety of diverse reagent-based assays in *the same instrument without the need for reconfiguration of the flow path,* simply, by adjusting the software script. We trust that these features along with the robustness and portability of the instrument will contribute to the acceptance of the new generation of Flow Injection technique by the oceanographic community.

Credit author statement

Mariko Hatta: Conceptualization; Methodology; Writing – original draft; Writing – review & editing, Jarda Ruzicka: Conceptualization; Methodology; Writing – original draft; Writing – review & editing, Chris I. Measures: Conceptualization; Methodology; Writing – original draft; Writing – review & editing, Madeline Davis: Conceptualization; Methodology; Writing – original draft; Writing – review & editing

Declaration of competing interest

The authors declare that they have no known competing financial interests or personal relationships that could have appeared to influence the work reported in this paper.

Acknowledgements

We would like to thank Graham Marshall, from Global FIA for design and fabrication of components supporting our research, and to Danielle Hull from the University of Hawaii S-LAB for providing LNSW. Financial support for this work came from the National Science Foundation grant # NSF-OCE 1924690 to MH. This is contribution no. 11301 of the School of Ocean Earth Science and Technology, University of Hawaii.

References

[1] J. Ruzicka, E.H. Hansen, Flow injection analyses: Part I. A new concept of fast continuous flow analysis, Anal. Chim. Acta 78 (1975) 145–157.
[2] J. Ruzicka, Redesigning flow injection after 40 years of development: flow programming, Talanta 176 (2018) 437–443.
[3] E.A.G. Zagatto, M.A.Z. Arruda, A.O. Jacintho, I.L. Mattos, Compensation of the Schlieren effect in flow-injection analysis by using dual-wavelength spectrophotometry, Anal. Chim. Acta 234 (1990) 153–160.
[4] I.D. McKelvie, D.M.W. Peat, G.P. Matthews, P.J. Worsfold, Elimination of the Schlieren effect in the determination of reactive phosphorus in estuarine waters by flow-injection analysis, Anal. Chim. Acta 351 (1997) 265–271.
[5] S. Auflitsch, D.M.W. Peat, P.J. Worsfold, S. Auflitsch, I.D. McKelvie, Determination of dissolved reactive phosphorus in estuarine waters using a reversed flow injection manifold†, Analyst 122 (1997) 1477–1480.
[6] P.J. Worsfold, R. Clough, M.C. Lohan, P. Monbet, P.S. Ellis, C.R. Quétel, G.H. Floor, I.D. McKelvie, Flow injection analysis as a tool for enhancing oceanographic nutrient measurements-A review, Anal. Chim. Acta 803 (2013) 15–40.
[7] E.H. Hansen, Database in "flow injection tutorial". http://www.flowinjectiontutorial.com/Database.html.
[8] J. Ruzicka, E.H. Hansen, Flow Injection Analysis, 2nd.Ed., J. Wiley & Sons, New York, 1988, p. p120. Ch. 3.
[9] https://www.flowinjectiontutorial.com/Theory%200.3.3.%20RTD%20Curves%20and%20FI%20Systems.html.
[10] J. Ruzicka, Lab-on-valve: universal microflow analyzer based on sequential and bead injection, Analyst 125 (2000) 1053–1060.
[11] https://www.flowinjectiontutorial.com/Methods%201.4.3.%20Miniaturized%20pFI%20Instrument.html.
[12] M. Hatta, J. Ruzicka, C.I. Measures, The performance of a new linear light path flow cell is compared with a liquid core waveguide and the linear cell is used for spectrophotometric determination of nitrite in sea water at nanomolar concentrations, Talanta 219 (2020) 121240.
[13] https://www.flowinjectiontutorial.com/Methods%201.4.12.%20Linear%20Light%20Path%20Flow%20Cell%20Construction.html.
[14] https://www.flowinjectiontutorial.com/Methods%201.4.7.%20In%20Search%20for%20an%20Ideal%20Pump.html.
[15] D.K. Wolcott, G.D. Marshall, Pulseless, reversible precision piston-array pump, USP 6 (2000) 79–313.
[16] M. Hatta, C.I. Measures, J. Ruzicka, Programmable Flow Injection. Principle, methodology and application for trace analysis of iron in a sea water matrix, Talanta 178 (2018) 698–703.
[17] M. Hatta, C.I. Measures, J. Ruzicka, Determination of traces of phosphate in sea water automated by programmable flow injection: surfactant enhancement of the phosphomolybdenum blue response, Talanta 191 (2019) 333–341.
[18] J. Ruzicka, G.D. Marshall, C.I. Measures, M. Hatta, Flow injection programmed to function in batch mode is used to determine molar absorptivity and to investigate the phosphomolybdenum blue method, Talanta 201 (2019) 519–526.
[19] C. Gal, W. Frenzel, J. Möller, Re-examination of the cadmium reduction method and optimisation of conditions for the determination of nitrate by flow injection analysis, Microchim. Acta 146 (2004) 155–164.
[20] E. Bishop, Pergamon Indicators, Press Oxford, in: D.R. Lide (Ed.), Also, CRC Handbook of Chemistry and Physics, CRC Press, Boca Raton, FL, 1978, p. 2008, 2007.
[21] J. Ma, L. Adornato, R.H. Byrne, D. Yuan, Determination of nanomolar levels of nutrients in seawater, TrAC Trends Anal. Chem. 60 (2014) 1–15.
[22] E.T. Steimle, E.A. Kaltenbacher, R.H. Byrne, In situ nitrite measurements using a compact spectrophotometric analysis system, Mar. Chem. 77 (2002) 255–262.
[23] W. Yao, R.H. Byrne, R.D. Waterbury, Determination of nanomolar concentrations of nitrite and nitrate in natural waters using long path length Absorbance spectroscopy, Environ. Sci. Technol. 32 (1998) 2646–2649.
[24] https://www.flowinjectiontutorial.com/Methods%201.2.37.%20pFI%20Single%20Reagent%20on%20Column%20Assay%20Nitrate.html.
[25] M.M. Grand, P. Chocholouš, J. Růžička, P. Solich, C.I. Measures, Determination of trace zinc in seawater by coupling solid phase extraction and fluorescence detection in the Lab-On-Valve format, Anal. Chim. Acta 923 (2016) 45–54.
[26] E.A. Nagul, I.D. McKelvie, P. Worsfold, S.D. Kolev, The molybdenum blue reaction for the determination of orthophosphate revisited: opening the black box, Anal. Chim. Acta 890 (2015) 60–82.
[27] J. Murphy, J.P. Riley, A modified single solution method for the determination of phosphate in natural waters, Anal. Chim. Acta 27 (1962) 31–36.
[28] https://www.flowinjectiontutorial.com/Methods%201.5.14.%20How%20to%20Optimize%20PMoB%20Assay.html.
[29] J. Thomsen, K.S. Johnson, R.L. Petty, Determination of reactive silica in sea water by flow injection analysis", Anal. Chem. 55 (1983) 2378–2382.
[30] J. Ma, R.H. Byrne, Flow injection analysis of nanomolar silicate using long pathlength absorbance spectroscopy, Talanta 88 (2012) 484–489.
[31] N. Amornthammarong, J.-Z. Zhang, Liquid-waveguide spectrophotometric measurement of low silicate in natural waters, Talanta 79 (2009) 621–626.
[32] M. Aoyama, K. Bakker, J. van Ooijen, S. Ossebaar, E.M.S. Woodward, Report from an International Nutrient Workshop Focusing on Phosphate Analysis. Texel, Netherlands, Royal Netherlands Institute for Sea Research, Netherland, 2012, ISBN 978-4-908583-01-8, 12-15 November 2012.
[33] S. Coverly, R. Kérouel, A. Aminot, A re-examination of matrix effects in the segmented-flow analysis of nutrients in sea and estuarine water, Anal. Chim. Acta 712 (2012) 94–100.